

## ITER ELM control requirements, ELM control schemes & required R&D

A. Loarte 1), D.J. Campbell 1), Y. Gribov 1), R.A. Pitts 1), N. Klimov 2), V. Podkovyrov 2), A. Zhitlukhin 2), I. Landman 3), S. Pestchanyi 3), B. Bazylev 3), J. Linke 4), T. Loewenhoff, G. Pintsuk 4), O. Schmitz 4), Y. Liang 4), T.E. Evans 5), M. Schaffer 5), M.E. Fenstermacher 5,6), M. Becoulet 7), G. Huysmans 7), E. Nardon 7), L. Baylor 8), J. Canik 8), R. Maingi 8), J.W. Ahn 8), B. Riccardi 9), G. Saibene 9), R. Sartori 9), M. Cavinato 9), T. Eich 10), M. Jakubowski 10), P.T. Lang 10), H. Thomsen 10), W. Suttrop 10), E. De la Luna 11), H. Wilson 12), A. Kirk 13)

- 1) ITER Organization, Route de Vinon sur Verdon, F-13115 Saint Paul lez Durance, France
- 2) SRC RF TRINITI, ul. Pushkovykh, vladenie 12, 142190, Troitsk, Moscow Region, Russia
- 3) Karlsruhe Institute of Technology, P.O. Box 3640, 76021 Karlsruhe, Germany (KIT)
- 4) Forschungszentrum Jülich GmbH, Association EURATOM-FZ Jülich, Institut für Energieforschung-Plasmaphysik, Trilateral Euregio Cluster, D-52425 Jülich, Germany
- 5) General Atomics, P.O. Box 85608, San Diego, California 92186-5608, USA
- 6) Lawrence Livermore National Laboratory, PO Box 808, Livermore, California, 94551 USA
- 7) CEA/IRFM, 13108 St Paul-lez-Durance, France
- 8) Oak Ridge National Laboratory, Oak Ridge, Tennessee 37831, USA
- 9) Fusion for Energy, ITER Department, Josep Pla, 2, Torres Diagonal Litoral B3, 08019 Barcelona, Spain
- 10) Association EURATOM-Max-Planck-Institut für Plasmaphysik, D-85748 Garching, Germany
- 11) Laboratorio Nacional de Fusión, Asociación EURATOM-CIEMAT, Madrid, Spain
- 12) University of York, Heslington, York YO10 5DD UK
- 13) EURATOM/CCFE Fusion Association, Culham Science Centre, Abingdon, OX14 3DB, UK

E-mail contact of main author: alberto.loarte@iter.org

**Abstract.** Control of ELM energy fluxes to plasma facing components is required for successful operation of ITER particularly in the high current/ $Q_{DT}$  scenarios. The basis for ELM energy losses in ITER is described as well as the requirements for ELM control including scenario integration issues. The status of the ELM control schemes which are being considered for ITER is reviewed together with the evaluation of possible alternative schemes.

### 1. Introduction

ITER operation in its high fusion performance DT scenarios (inductive, hybrid and steady-state) relies on the achievement of the H-mode confinement regime with  $H_{98} \geq 1$  and a significant plasma pressure gradient at the plasma edge which is expected to lead to the triggering of ELMs. Operation of ITER with H-mode plasmas is also foreseen during the non-active (H & He) phases and during DD operation. This will allow the study of the features of H-mode plasmas at the ITER scale and to develop scenarios for DT operation in ITER during them, including ELM control schemes. ELM control requirements for ITER have been derived on the basis of a combination of empirical extrapolation and modelling of both the characteristics of ELM power fluxes in present experiments and the behaviour of the ITER plasma-facing materials under ELM transient loads in the ITER Members' tokamaks and research facilities/institutions. On the basis of these requirements, various schemes to achieve them are being considered for ITER all of which are the subject of on-going R&D in the ITER Members' research programmes. This paper reviews the basis for the ELM control requirements in ITER, ELM control schemes being considered for ITER and discusses the outstanding R&D issues for their application in ITER. Alternative control schemes are also briefly described.

### 2. ITER ELM energy fluxes to plasma facing components and control requirements

#### 2.1. Expected ELM energy loads on ITER plasma facing components

The expected energy loads on ITER plasma-facing components (PFCs) are determined by the magnitude and temporal characteristic of the energy losses from the main plasma and the transport of this energy to the material surfaces. ELM energy losses in present experiments have been found to be well correlated with the neoclassical pedestal plasma collisionality  $v_{ped}^*(neo)$ ;  $\Delta W_{ELM}/W_{ped} = 0.07 [v_{ped}^*(neo)]^{0.3}$ , which predicts an ELM energy loss of  $\Delta W_{ELM} \sim 20$  MJ for the expected pedestal plasma conditions in the ITER  $Q_{DT} = 10$  regime [Loarte03a, PIPB07a]. Measurements of the average power flux carried by ELMs ( $P_{ELM}$ ) show that this is typically in the range  $P_{ELM} = (0.2-0.4) P_{sep}$ , where  $P_{sep}$  is the power crossing the separatrix [PIPB07a]. Applying this to ITER  $Q_{DT} = 10$  conditions, for which  $P_{sep} \approx 100$  MW, provides a "natural" or uncontrolled ELM frequency of  $f_{ELM}^{uncontrolled} = 1 - 2$  Hz. The reduction in ELM size with collisionality is mainly due to the reduction of the perturbation to the plasma

temperature profiles by ELMs rather than to a reduction of the density perturbation [Loarte03a]. This has been recently reproduced by non-linear MHD simulations of the ELM event including the transport of plasma energy to the PFCs for low resistivity/collisionless edge plasma conditions [Pamela10a], providing a firmer physics basis for this empirical scaling. Despite these encouraging theoretical advances, a complete physics basis to extrapolate ELM energy losses from present experiments to ITER is still lacking. Further experimental and theoretical R&D is needed to identify the processes causing the deviations from the collisionality scaling (higher and lower values) observed in some experimental conditions and to improve predictions for the magnitude of the ELM energy loss in ITER.

Analysis of experimental measurements in tokamaks indicates that a significant amount of the energy lost by the plasma during ELMs reaches the PFCs in localised areas, in particular near the divertor target separatrix [Eich03a]. An upper limit for the ELM energy fluxes at the ITER divertor is thus derived by assuming that the effective area for ELM energy deposition will be similar to that between ELMs; namely  $\lambda_{q\text{-midplane}}^{\text{ELM}} = 5 \text{ mm}$  for the 15 MA  $Q_{\text{DT}} = 10$  scenario, where  $\lambda_{q\text{-midplane}}^{\text{ELM}}$  is the effective fall-off length for ELM energy deposition at the divertor mapped to the outer midplane [PIP07a]. On the basis of experimental data [PIP07a] and the expected pedestal plasma parameters in ITER with  $Q_{\text{DT}} = 10$ , the ELM energy pulse at the divertor is expected to have a rise and decay phases of typical duration of  $\tau_r = 250\text{-}500 \mu\text{s}$  and  $\tau_d = (1\text{-}2) \tau_r$  respectively, values which bound the lower limits found in experiments [Eich09a, Eich10a]. Similarly, experiments show that energy deposition during ELMs at the inner and outer divertor targets is usually asymmetric with more energy ( $\sim$  factor of 2) reaching the inner divertor for discharges with the favourable direction of the toroidal field for H-mode access [Eich07a] as adopted for ITER operation, thus a maximum ratio of 2 for the ELM energy reaching the inner divertor to that of the outer divertor is assumed for ITER. Power fluxes at the ITER PFCs castellated structures during ELMs are strongly affected by kinetic effects since the expected typical Larmor radius of ions impacting at the ITER divertor during an ELM (with energies of up to several keVs) is in the mm range and thus comparable with or larger than the separation between consecutive macro brush elements ( $\sim 0.5 \text{ mm}$ ). As a consequence, for the typical impact angles of field lines at the ITER divertor strike points of  $2\text{-}3^\circ$ , the energy fluxes on the exposed macrobrush edges ( $\sim 90^\circ$  impact angle) are expected to be only a factor of 2 larger than on the front surface of the brush [Dejarnac09a], instead of a factor of 20-30 expected from geometric arguments.

Recent experimental evidence from DIII-D [Jakubowski09] and JET [Eich10a] has shown that the effective area for ELM energy deposition ( $A_{\text{ELM}}$ ) is itself dependent on the magnitude of the ELM energy loss. For small  $\Delta W_{\text{ELM}}$ ,  $A_{\text{ELM}}$  is indeed similar (a factor of 1.0-1.5) to that between ELMs, as assumed in the derivation of the upper limit for ELM energy flux at the ITER divertor. However, for larger  $\Delta W_{\text{ELM}}$ ,  $A_{\text{ELM}}$  can be significantly larger (by factors of up to 3-4) than its inter-ELM value so that the peak ELM energy flux at the divertor decreases more weakly than  $\Delta W_{\text{ELM}}$  with decreasing ELM size. Experimental characterisation of  $A_{\text{ELM}}$  itself is a complex issue since the ELM heat flux footprint changes in time during the ELM [Thomsen10a]; similarly the physics basis for extrapolation of  $A_{\text{ELM}}$  to ITER remains uncertain. Despite these uncertainties, as described below, the finding of the change of  $A_{\text{ELM}}$  with  $\Delta W_{\text{ELM}}$  has implications both for the range of plasma parameters (principally the plasma current  $I_p$ ) at which ITER will be able to operate without active ELM control and on the level of ELM control required for the various levels of  $I_p$ . Further R&D is required to quantify the magnitude of these implications for ELM energy fluxes at the ITER divertor and first wall.

## 2.2. Divertor plasma facing materials behaviour under ELM-like transient loads

Experiments have been performed in plasma gun facilities (such as QSPA in Troitsk [Zhitlukhin07a, Klimov09a]) and electron beams (such as Judith and Judith-II in FZJ [Linke08a]) to expose divertor target components with ITER-like materials/specifications to transient loads similar to those expected during ELMs in ITER, including the ratio of edge to front surface macrobrush energy deposition (in QSPA). On the basis of these results, a maximum energy flux of  $0.5 \text{ MJm}^{-2}$  on the front face of the macrobrush has been adopted as the upper limit for allowed ELM energy loads on the ITER divertor without a major reduction of the divertor lifetime (i.e. controlled ELMs). For this maximum allowed load, CFC erosion is very limited and large scale melting of W is avoided both on the front face and edges of the macro-brushes. Exceeding this value by a factor of 2-3 (i.e.  $1.0\text{-}1.5 \text{ MJm}^{-2}$ ) leads to CFC

erosion rates of  $\sim 1 \mu\text{m}/\text{ELM}$  and to macroscopic scale  $W$  melting with possible ejection of droplets [Zhitlukhin07a, Klimov09a]. An erosion rate of this magnitude would require that the divertor target be replaced every  $\sim 10^4$  ELMs to be compared with  $\sim 1\text{-}2 \text{ ELM s}^{-1}$  expected for  $Q_{\text{DT}} = 10$ . In addition to this divertor lifetime issue, it is also important to note that the quantity of target material eroded by every of ELM of this magnitude is in the range of grams. If a significant proportion of this materials enters the confined plasma, it is likely to cause a significant transient increase of the plasma  $Z_{\text{eff}}$  and plasma radiation leading to deterioration of plasma performance (as seen, for example at JET for large ELMs [Pitts09a, Huber10a]), if not a disruptive radiative plasma collapse. Maintaining ELM energy loads to PFCs under damage thresholds is therefore mandatory for reliable high performance operation in ITER.

An important outstanding issue is the possible enhancement of erosion and/or degradation of PFC power handling performance associated with thermal fatigue effects by a large number of events with energy fluxes under the damage threshold value of  $\sim 0.5 \text{ MJm}^{-2}$ . Experiments have been recently performed to address this concern in which the number of exposures with energy fluxes  $\sim 0.5 \text{ MJm}^{-2}$  has been increased up to 500 in the plasma gun QSPA [Klimov10a, Riccardi10a], and in the range of  $10^3 - 10^5$  pulses with energy fluxes  $\sim 0.2 \text{ MJm}^{-2}$  in the electron beam experiment Judith-II [Loewenhoff10a]. The QSPA experiments have shown that already at energy fluxes of  $\sim 0.5 \text{ MJm}^{-2}$  erosion of the CFC PAN fibres can reach values of up to  $\sim 0.15 \mu\text{m}$  per ELM-like event as shown in Fig. 1 [Klimov10a, Riccardi10a], although it is not clear if such erosion rate would be maintained once the pitch fibres start to receive a larger fraction of the transient load following erosion the PAN fibres.

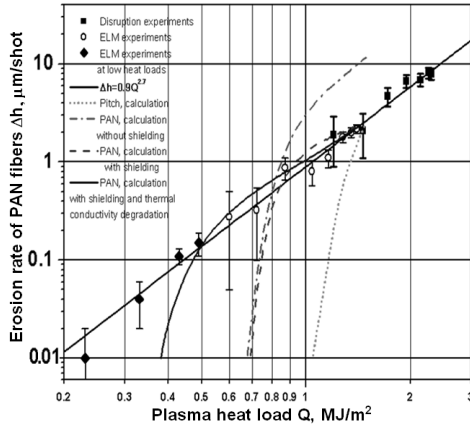


Figure 1. Experimental and numerical estimation of the erosion rate of PAN fibres [Klimov10, Riccardi10 & references therein] extent that the acceptable divertor load for controlled ELMs would need to be reduced under the present limit  $0.5 \text{ MJm}^{-2}$ .

For  $W$  components, roughening and cracks of the front macrobrush surface are observed at the energy densities explored both for the QSPA experiments [Klimov10a, Riccardi10a] and the Judith-II experiments [Loewenhoff10a] (typical roughness in the  $\mu\text{m}$  scale). Neither the change of surface morphology in  $W$  nor the small erosion on PAN fibres for CFC degrade the performance of the divertor component for stationary power fluxes at the level of  $\sim 10 \text{ MWm}^{-2}$  required in ITER, in comparison to that of components not exposed to ELM loads [Riccardi10a]. Further R&D is ongoing to determine whether high numbers of cycles affect material surface damage/erosion to an

### 2.3. ELM control requirements in ITER

The requirement on the acceptable maximum energy density during controlled ELMs of  $0.5 \text{ MJm}^{-2}$  for an ELM power waveform with rise time of  $\tau_r = 250\text{-}500 \mu\text{s}$  and decay time  $\tau_d = (1\text{-}2) \tau_r$ , as expected for the pedestal plasma conditions at  $15 \text{ MA } Q_{\text{DT}} = 10$ , can be transformed into an upper limit for the maximum energy loss during controlled ELMs in ITER for a range of plasma currents. For  $15 \text{ MA } Q_{\text{DT}} = 10$ , this corresponds to ELMs with  $\Delta W_{\text{ELM}} \sim 0.7 \text{ MJ}$  with a frequency of  $f_{\text{ELM}}^{\text{controlled}} \sim 30 - 60 \text{ Hz}$ . The allowed upper limit for controlled ELM energy loss for various levels of  $I_p$  is compared with that expected for uncontrolled ELMs (Sect. 2.1) in Fig. 2 for constant or varying  $q_{95}$ , under the assumption that  $A_{\text{ELM}}$  scales  $\sim 1/I_p$  and that pedestal temperature and density scale approximately linearly with  $I_p$  as seen in experiments/modelling [Snyder09]. Two cases are considered: one in which  $A_{\text{ELM}}$  is similar to the inter-ELM wetted area and the other in which  $A_{\text{ELM}}$  is 4 times larger, which covers the range of experimental observations [Jakubowski09a, Eich10a]. Depending on the broadening of the ELM energy flux footprint for uncontrolled ELMs in ITER, Fig.2 shows that “natural” or “uncontrolled” ELM energy losses are acceptable for the divertor targets for  $I_p$  in the range of  $6 - 9.5 \text{ MA}$ . In fact, because  $A_{\text{ELM}}$  is observed to decrease with  $\Delta W_{\text{ELM}}$ , the consequences of this new experimental finding affect more significantly the expected energy fluxes for uncontrolled or partially controlled ELMs (with  $\Delta W_{\text{ELM}} < \Delta W_{\text{ELM}}^{\text{uncontrolled}}$ ) than the

requirements to achieve fully controlled ELMs at high  $I_p$ , for which very small or no broadening is expected, as shown in Fig. 3.

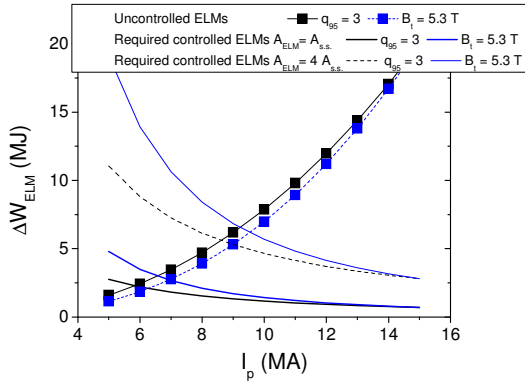


Figure 2. Expected main plasma ELM energy loss ( $\Delta W_{ELM}$ ) for uncontrolled ELMs and required for controlled ELMs in ITER versus plasma current ( $I_p$ ) for a range of assumptions concerning the effective area for ELM energy deposition ( $A_{ELM}$ ) and two assumptions regarding the change of safety factor with  $I_p$  (constant  $q_{95}$  or constant  $B_p$ ).

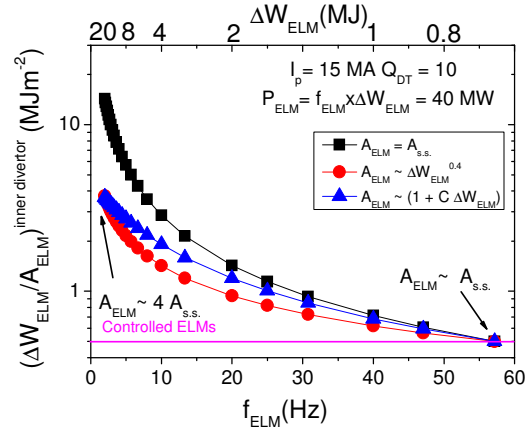


Figure 3. Expected ELM energy flux at the inner divertor ( $\Delta W_{ELM}/A_{ELM}$ ) in ITER versus ELM frequency ( $f_{ELM}$ ) or ELM size ( $\Delta W_{ELM}$ ) for various assumptions regarding the dependence of the effective area for ELM energy deposition ( $A_{ELM}$ ) on  $\Delta W_{ELM}$ .

The control of ELM energy fluxes to PFCs needed in ITER must be maintained simultaneously with other scenario constraints required to achieve high  $Q_{DT}$  operation as well as to maintain control of the stationary power fluxes to PFCs. Some key scenario compatibility issues to be addressed when considering any ELM control scheme in ITER are :

- Effects on average pedestal pressure and consequences for plasma energy confinement
- Effects on confined plasma transport and consequences for fuelling of ITER plasmas
- Effects on stationary edge power/particle fluxes and radiative divertor operation for adequate power handling and erosion control.
- Effects on access to high confinement regimes.

### 3. ELM control schemes being considered for ITER and required R&D

Control of ELM energy losses in ITER scenarios is envisaged by the application of schemes specifically designed for this purpose (currently pellet pacing and ELM control coils) and by the use for ELM control, within their technical capabilities, of systems designed for other purposes (vertical kicks with the in-vessel vertical stability coils, edge ECRH heating, etc.) New schemes for ELM control could be integrated in ITER as possible future upgrades but probably only if they are port-based systems.

#### 3.1. ELM control by pellet pacing

Injection of solid frozen hydrogenic pellets is considered in ITER to trigger ELMs based on results from present experiments. Such triggering is driven by the local plasma pressure perturbation caused by the pellets, which ultimately drives an MHD instability at the plasma edge causing the ELM [Huysmans10a]. For high enough pellet frequencies (compared to the natural ELM frequency), all ELMs in the discharge can be triggered by pellets, i.e. ELM pacing by pellets [Lang04b]. To first order, pellet-paced ELM energy losses are found to scale as  $\sim 1/f_{ELM}$  so that to meet ITER ELM control requirements for the  $Q_{DT} = 10$  scenario a pellet injection frequency of  $\sim 30 - 60$  Hz is required. This can be met by the parallel use of various high field side and low field side injectors foreseen for ITER each with a maximum repetition frequency of 16 Hz. Previous experiments with fuelling pellets had demonstrated an increase of  $f_{ELM}$  from its ‘natural’ value by a factor  $\sim 2-3$  with moderate consequences for plasma confinement [Lang04b]. The increase was limited either by hardware (limit of pellet injection frequency, etc.) or by the excessive over-fuelling of the plasma associated with the pellet pacing, which was performed with injectors have so far been optimised for plasma fuelling in present devices. More recent experiments in DIII-D have achieved an enhancement factor of 5

above the natural ELM frequency with negligible plasma fuelling and a moderate decrease of  $\sim 10\%$  in plasma confinement [Baylor10a], although  $\sim 50\%$  of the ELMs in these experiments were not triggered by the pellets themselves. ELM control by pellet pacing has been shown to be compatible with some of the requirements for ITER operation. For instance, on ASDEX Upgrade pellet pacing has been shown to be compatible with the high radiation regimes required to ensure acceptable stationary power fluxes on the ITER divertor targets [Lang05a].

The major uncertainties regarding the application of this ELM control scheme to ITER are related to : a) the pellet size which is required to trigger an ELM and the associated particle throughput required for ELM control, b) the degradation in energy confinement associated with the increase of  $f_{\text{ELM}}$  by a factor of  $\sim 30$  with respect to its “uncontrolled” value and c) pellets-specific effects on the deposition of ELM energy on PFCs. Triggering requirements for ELMs in ITER have been set conservatively by assuming that the pellet needs to reach the top of the pedestal plasma in ITER and provide there a minimum size of the density perturbation as derived from experimental observations [Gál08a]. For the design velocities of the ITER pellet injector (300-500m/s), the required pellet content for ELM triggering from these calculations is estimated to be in the range  $1\text{-}4 \times 10^{21}$  particles/pellet ( $\sim 15\text{-}66 \text{ mm}^3$ ) which is within the range foreseen for the ITER injector ( $17\text{-}92 \text{ mm}^3$ ) [Maruyama10a]. Because of their shallow penetration, the fuel injected by ELM pacing pellets is expected to be expelled by the triggered ELMs and not to contribute significantly to the core plasma fuelling. Nevertheless, this is expected to cause a significant contribution to the total plasma particle throughput; e.g. pellets with  $2 \times 10^{21}$  particles/pellet injected at 30 Hz for ELM control provide an outflow of  $\sim 6 \times 10^{22} \text{ s}^{-1}$  or  $120 \text{ Pam}^3 \text{ s}^{-1}$  which is 60% of the maximum average throughput for the  $Q_{\text{DT}} = 10$  inductive [Kukushkin10a]. Evidence from time of flight measurements in DIII-D [Baylor10b] indicates that there is margin to reduce the ITER requirement regarding pellet penetration for ELM triggering in ITER as shown in Fig. 4 [Baylor10b, Lang10a]. Recent results from JET and modelling based on them indicate that ELM triggering may be achievable in ITER with pellets containing  $\sim 7.5 \times 10^{20}$  particles [Garzotti10a]. On the other hand, very small pellets that penetrate the plasma by only few mm in JET are found not to trigger ELMs [Alper10a] indicating that besides penetration there is a minimum perturbation size required for a pellet to trigger an ELM as expected from MHD modelling [Huysmans10a]. Further experiments with small pellets in a pacing regime in conditions closer to ITER together with modelling are required to provide more accurate predictions for ITER. Similarly the effect of ELM control by pellet pacing on plasma confinement has only been assessed up to moderate enhancements of the ELM frequency ( $< 5$ ) [Lang04b, Baylor 10a]. Further experiments with smaller pellets (to minimize pellet induced losses) and higher frequency enhancements ( $> 10$ ) are required to determine the confinement degradation to be expected in ITER by the application of this control technique. Finally, ELM triggered pellets are seen to lead to the preferential expulsion of plasma energy in one or few filaments depositing on the PFCs [Wenninger10a], as expected from modelling [Huysmans10a], albeit for fuelling-like pellets. It is important to understand how these local pellet-paced ELM fluxes depend on pellet size and pedestal plasma characteristics in order to determine if they could be lead to additional local erosion at the ITER PFCs.

### 3.2. ELM control by edge magnetic field perturbation

The application of perturbations to the edge magnetic field in tokamaks has been seen to affect ELM behaviour in several tokamak devices [Fenstermacher10a and references therein]. As demonstrated in DIII-D for ITER-like plasmas [Evans08a], it is presently the only active ELM control technique with the potential to achieve complete ELM suppression. Its implementation in ITER is being considered by means of independently powered in-vessel ELM control coils, 3 per vessel sector above, below and around the outer midplane (Fig. 5.a). The physics processes that lead to the changes in ELM behaviour (and their eventual suppression) and the associated implications for the application of this technique in ITER remain uncertain and are the subject of active research in the various tokamak devices and under ITPA coordinated activities [Fenstermacher10a]. The specifications of the ITER ELM control coil system with regards to maximum current capability and flexibility have therefore been derived on the basis of empirical guidelines from ELM suppression experiments in DIII-D [Fenstermacher08a]. A Chirikov island overlap parameter (calculated from vacuum

perturbation field)  $\sigma_{\text{chir}} > 1$  on all magnetic surfaces from normalized poloidal flux  $\psi = 0.835$  outwards and the need to achieve a good alignment of the perturbation with the field line pitch (i.e. a resonant perturbation) are requirements for the ITER design. To account for uncertainties, a 20% margin in coil current is taken into the ITER design whose maximum

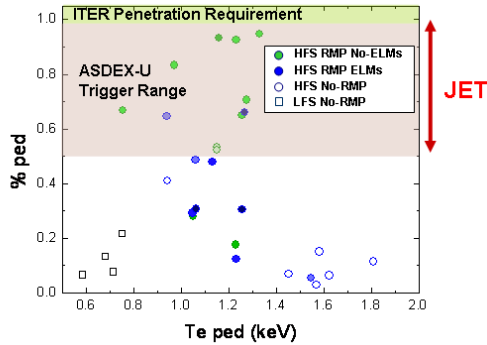


Figure 4. Measured pellet penetration normalised to the distance from separatrix to pedestal top at which ELMs are triggered for a series of plasma and launching geometries (HFS and LFS) in DIII-D versus pedestal temperatures [Baylor10b]. For comparison the pellet penetration at which ELM triggering is observed in JET and ASDEX-Upgrade are shown [Lang10a].

current capability is 90 kAt per coil leading to a resonant edge magnetic field perturbation in the pedestal region for 15 MA  $Q_{DT} = 10$  plasmas of  $\sim 6.6 \cdot 10^{-4} \times B_{t,0}$  [Schaffer10a], where  $x B_{t,0}$  is the toroidal magnetic field on axis. Recent multi-machine experiments have shown in fact that achieving the above Chirikov island overlap criteria is not sufficient to obtain ELM suppression in other devices than DIII-D [Fenstermacher10a]. On the other hand significant reductions in ELM size (by  $\sim 4-5$ ) are obtained in several devices, such as JET, when good alignment between the applied perturbation and the field line pitch is obtained at values of the resonant perturbation a factor of 2-3 lower than those achievable in ITER and a very weak level of edge ergodisation [Liang10b]. This supports the ITER design

guideline with regard to field perturbation magnitude and power supply flexibility.

A number of physics and scenario integration issues remain outstanding concerning the application of this technique to ITER. These are the subject of active experimental and theoretical research and can only briefly mentioned here : a) the effect of plasma shielding of the magnetic field perturbation and the consequences for ELM mitigation/suppression in ITER plasma conditions, b) the effects on plasma performance and ITER operation of the non-resonant components of the applied magnetic perturbation, c) the physics processes affecting edge plasma particle transport with edge magnetic field perturbations and the consequences for ITER plasma fuelling and fuelling schemes (including ELM control/suppression with pellet fuelling), d) the effects of the edge magnetic field perturbations on the access to H-mode and  $H \sim 1$  conditions for edge power flow close to the expected L-H transition power (as foreseen for  $Q_{DT} = 10$  operation in ITER), e) the compatibility of ELM control/suppression by edge magnetic field perturbation with radiative divertor operation and low stationary power fluxes to plasma facing components, etc.

While the importance and consequences of the above issues remain uncertain for ITER, the ELM control coil system has been designed to account for several of them to some level by the introduction of appropriate flexibility. For example, the application of edge magnetic field perturbations is seen in some experiments to produce toroidally asymmetric structures in the divertor particle and power fluxes [Jakubowski09a, Ahn10a, Schmitz08a]. While the evaluation of the magnitude of these fluxes and their consequences for ITER operation remain uncertain, they may lead to excessive net erosion rates at the ITER divertor due to the decrease of re-deposition in these areas. The ITER ELM control coil system is therefore being designed to be capable of slowly rotating the perturbation to smooth out the effects of these toroidally localised fluxes while avoiding excessive thermal cycling of the ITER divertor components. Modelling of the thermal behaviour of ITER divertor components [Komarov09a] has shown that that with a rotation frequency of the power flux pattern of at least 1 Hz no thermal cycling effects are expected even for the worst case considered (power fluxes of  $20 \text{ MWm}^{-2}$  in the toroidally asymmetric power deposition areas). On this basis a maximum frequency of 5 Hz has been adopted for the modulation of the current in the ITER ELM control coils which are expected to be used with  $n = 4$  (or  $n=3$ ) toroidal phasing (power/particle flux pattern rotation frequency of  $5\text{Hz}/n$ ). This capability can be applied to ramp the edge magnetic field perturbation from zero to its maximum strength in a time interval as short as 50 ms thus allowing the application of the perturbation after the transition

to H-mode has taken place avoiding possible negative effects of the edge magnetic field perturbation on the dynamics and threshold power of this transition.

An important practical issue with regards to the capability for ELM control provided by the proposed ITER coil set is the quantification of the performance of the system as a whole in the case of malfunction of one or more coils. This has been performed by means of an analytical approximation for the magnetic field created by ITER ELM control coil system [Schaffer10a], benchmarked with numerical modelling [Schaffer10b], by evaluating the capability of the system with malfunctioning coils to meet its design criteria for ELM suppression (i.e. Chirikov island overlap  $\geq 1$  for  $\psi_N \geq 0.835$ ) [Loarte10a] for various levels of  $I_p$ . In this evaluation, it is assumed that meeting the above design criterion ensures ELM suppression in ITER for a given  $I_p$  and the probability of the coil system with  $n$  failed coils to meet this criterion is evaluated as  $\sim N_{\text{fail}}^{\text{crit-met}}(n)/N_{\text{fail}}(n)$ , where  $N_{\text{fail}}$  is the total number of possible cases with  $n$  failed coils and  $N_{\text{fail}}^{\text{crit-met}}$  is the number of them for which the edge magnetic perturbation produced is sufficient to meet the design criterion for that  $I_p$ . The results of this assessment for up to 3 malfunctioning coils and both for stationary and rotating edge magnetic field perturbations are summarised in Fig. 5.b. As shown in this figure, the need to rotate the perturbation increases the degradation of the system performance since in this case at some point of the rotation cycle the current in one or various of the malfunctioning coils is required to be maximum (in absolute value) for which no current can be applied. In the case of a stationary perturbation, the toroidal phase of the currents applied to the coils can be adjusted to minimise the effect of the malfunctioning coils thus reducing to a negligible level the consequences of an individual coil failure. On the basis of this analysis it can be concluded the capability for ELM suppression of the ITER ELM control coil set is maintained for plasma currents above 14.5 MA for the vast majority of cases in which up to 3 coils malfunction.

**3.3. Alternative ELM control schemes in ITER**

As mentioned before, although not a requirement for their design, some of the ITER systems can be applied to control ELMs following demonstration in present experiments. Present evidence shows that some of these alternative schemes are unlikely to provide a viable solution for the control of ELMs in the flat top of the  $Q_{DT}=10$  scenario but, despite this, their application may be viable for lower  $I_p$  scenarios or to low  $I_p$  phases of the  $Q_{DT} = 10$  scenario. The capabilities of these schemes are briefly summarised below :

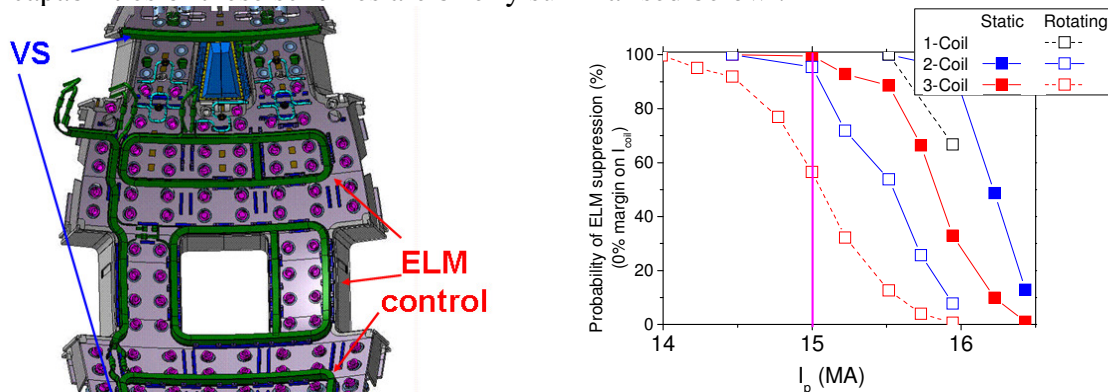


Figure 5.a. Layout of the proposed in-vessel coils for vertical stability and ELM control in ITER.

Figure 5.b. Cumulative probability for ELM suppression for  $n$  (1, 2, 3) malfunctioning coils in ITER versus plasma current for static and rotating perturbations

a) ELM control by vertical plasma movements. This technique has been demonstrated in various tokamaks [Degeling03a, Lang04a, Gerhardt10a, Hughes10a, Sartori08a] and extensively studied at JET [de la Luna09a]. The capabilities for vertical plasma movements by utilizing the in-vessel vertical stability coils has been assessed for the ITER  $Q_{DT} = 10$  scenario and found to be very limited (peak to peak centroid displacement of  $\sim 2-3$  cm) for high frequencies in the range of 30-60 Hz as required for successful ELM control; mainly because of overheating of the coils themselves, and a possible increased risk of worsening plasma vertical stability control [Gribov10a, Cavinato10a]; which is much lower than expectations from empirical extrapolations to ITER ( $\sim 6$  cm). Therefore ELM control with this scheme

does not appear to be viable for  $Q_{DT} = 10$  plasma conditions, although its use for lower  $I_p$  phases of this scenario and lower  $I_p$  plasmas in ITER seems more promising [Cavinato 10a].

b) *ELM control by edge heating and current drive*. Modification of the ELM and pedestal plasma behaviour by use of edge ECRH has been observed in some experiments [Horton04a, Oyama08a], but the physics basis for these modifications, their magnitude and extrapolation to ITER as well as issues of practical implementation (risk to in-vessel components, etc.) remain outstanding. Use of ECRH deposition at the plasma edge is possible up to injected powers of 7 MW out of 20 MW with the upper launcher design [Henderson&Saibene09a] thus allowing the test of this control approach in ITER. Other novel ideas such as the control of modes similar to the edge harmonic oscillation for ELM control by interaction with ICRH waves at the plasma edge need careful consideration for implementation in ITER following successful experimental demonstration.

#### 4. Conclusions

Control of ELM energy fluxes to PFCs in ITER is required for reliable operation in high  $I_p/Q_{DT}$  scenarios. Improved quantification of the requirements for ELM control for ITER operation requires further experimental and theoretical R&D on the physics processes leading to ELM energy losses and the transport of this energy to PFCs in addition to the behaviour of PFCs subject to these transient loads. Active ELM control schemes presently foreseen for ITER are based on the two techniques that have provided most promising results in present devices : pellet pacing and edge magnetic field perturbation. While the design of both systems for ITER are based on guidelines from experiments and modelling, significant uncertainties remain with respect to their application in ITER. A focused R&D programme is being carried out by the ITER Members's research facilities in coordination with the ITER Organization, ITPA and Domestic Agencies to address these uncertainties as well as to evaluate/develop alternative methods for ELM control applicable to ITER plasma/device conditions.

**Disclaimer:** The views and opinions expressed herein do not necessarily reflect those of the ITER Organization.

#### 5. References

- [Ahn10a] Ahn, J.-W., et al, Nucl. Fusion **50** (2010) 045010.  
 [Alper10a] Alper, B., et al., Proc 37<sup>th</sup> EPS Conference, Dublin, Ireland, 2010.  
 [Baylor10a] Baylor, L., et al., Proc 37<sup>th</sup> EPS Conference, Dublin, Ireland, 2010.  
 [Baylor10b] Baylor, L., et al., 18<sup>th</sup> ITPA Pedestal Group Meeting, Naka, Japan, 2010.  
 [Cavinato10a] Cavinato, M., Private Communication  
 [de la Luna09a] de la Luna, 51<sup>st</sup> APS Conf., Atlanta, USA, 2009.  
 [Degeling03a] Degeling, A.W., et al, Plasma Phys. Control. Fusion **45** (2003) 1637.  
 [Dejarnac09a] Dejarnac, R., et al., J. Nucl. Mater. **390 -391**, (2009) 818.  
 [Eich03a] Eich, T., et al., Physical Review Letters **19** (2003) 5003.  
 [Eich07a] Eich, T., et al., J. Nucl. Mater. **363-365** (2007) 989.  
 [Eich09a] Eich, T., et al., J. Nucl. Mater. **390 -391**, (2009) 760.  
 [Eich10a] Eich, T., et al., Proc. 19<sup>th</sup> PSI Conference, San Diego, USA, 2010.  
 [Evans08a] Evans, T. E. et al., Nucl. Fusion **48** (2008) 024002.  
 [Fenstermacher 2008a] Fenstermacher, M.E., et al, 2008 Phys. Plasmas **15** 056122  
 [Fenstermacher10a] Fenstermacher, M., et al, this conference.  
 [Gál08a] K. Gál et al, Proc. 22<sup>nd</sup> IAEA Fusion Energy Conf. (2008) TH/P4-5.  
 [Garzotti10a] Garzotti, L., et al., Proc 37<sup>th</sup> EPS Conference, Dublin, Ireland, 2010.  
 [Gerhardt10a] Gerhardt, S., et al, Nucl. Fusion **50** (2010) 064015.  
 [Gribov10a] Gribov, Y., et al., [Assessment of capability of VS in-vessel coils to mitigate ELMs by plasma vertical displacements \(32JRAU\)](#)  
 [Henderson&Saibene09a]. Henderson, M. and Saibene, G., Upper Launcher CDR Report, 2009.  
 [Horton04a] Horton, L., et al., Plasma Phys. Control. Fusion **46** (2004) B511.  
 [Huber10a] Huber, A., et al., Proc. 19<sup>th</sup> PSI Conference, San Diego, USA, 2010.  
 [Hughes09a] Hughes, J., ITPA Pedestal Meeting, Princeton, 2009.  
 [Hughes10a] Hughes, J., ITPA Pedestal Meeting, Naka, 2010.  
 [Huysmans10a] Huysmans, G., et al., Proc 37<sup>th</sup> EPS Conference, Dublin, Ireland, 2010.  
 [Jakubowski09a] Jakubowski, M.W., et al., Nucl. Fusion **49** (2009) 095013.  
 [Klimov10a] Klimov, N., et al., Proc. 19<sup>th</sup> PSI Conference, San Diego, USA, 2010.  
 [Komarov09a] Komarov, V., et al., [Thermal Analysis of monoblock caused by ELM coils 15 March 2009 v1 \(2NGS76\)](#)  
 [Kukushkin10a] Kukushkin, A., et al., Proc. 19<sup>th</sup> PSI Conference, San Diego, USA, 2010.  
 [Lang04a] Lang, P.T., et al, Plasma Phys. Control. Fusion **46** (2004) L31.  
 [Lang04b] Lang, P.T., et al, Nucl. Fusion **44** (2004) 665.  
 [Lang05a] Lang, P.T., et al, Nucl. Fusion **45** (2004) 502.  
 [Lang10a] Lang, P., T., et al., 18<sup>th</sup> ITPA Pedestal Group Meeting, Naka, Japan, 2010.  
 [Linke08a] Linke, J. et al 2008, in Proc. of the World Academy of Ceramics – FORUM 2008, Ceramic Materials in Energy Systems for Sustainable Development, Chianciano Terme, Italy, 2008.  
 [Loarte 03a]Loarte, A. et al Plasma Phys. Control. Fusion **45** (2003) 1549.  
 [Loarte10a] Loarte, A., et al., [Initial evaluation of limitations to ELM suppression in ITER associated with failure of ELM coils \(339RLD\)](#)  
 [Loewenhoff10a] Loewenhoff, T., et al., Proc. 19<sup>th</sup> PSI Conference, San Diego, USA, 2010.  
 [Maruyama10a] Maruyama, S., et al., this conference.  
 [Oyama08a] Oyama, N., Pedestal ITPA meeting, Milan, 2008.  
 [Pamela10a] Pamela, S., et al., Proc 37<sup>th</sup> EPS Conference, Dublin, Ireland, 2010.  
 [PIPB07a] Progress in the ITER Physics Basis **47** (2007) S1.  
 [Pitts09a] Pitts, R., et al., J. Nucl. Mater. **390 -391**, (2009) 755.  
 [Riccardi10a] Riccardi, B., et al., Proc. 19<sup>th</sup> SOFT Conference, Porto, Portugal, 2010.  
 [Sartori08a] Sartori, F., et al, Proc. 35<sup>th</sup> EPS Conf. on Plasma Phys., Vol **32D** (2008) P-5.045.  
 [Schaffer10a] Schaffer, M., et al., [Degradation of RMP Harmonics by Failed ELM Control Coils in ITER \(35CYUN\)](#)  
 [Schaffer10b] Schaffer, M., et al., [Numerical Benchmark of an Analytic Model of Resonant Harmonic Degradation Due to Failure of a Few ITER ELM Coils \(358PB8\)](#)  
 [Schmitz08a] Schmitz, O., et al., Plasma Phys. Controlled Fusion **50** (2008) 124029.  
 [Snyder09a] Snyder, P., et al, Nucl. Fusion **49** (2009) 085035.  
 [Thomsen10a] Thomsen, H., et al., this conference.  
 [Zhitlukhin07a] Zhitlukhin et al, J. Nucl. Mater. **363-365**, (2007) 301.  
 [Wenninger10a] Wenninger, R., et al., Proc 37<sup>th</sup> EPS Conference, Dublin, Ireland, 2010.